Note added in proof. It has come to the attention of the authors that Ivanov *et al.*[24] have recently reported observing a polarization signal from (100)-oriented NaCl shocked in the 50 to 550 kbar range. Their results are in general agreement with those reported above—the polarization signal changed sign from positive to negative at 100–150 kbar and approached zero at 550 kbar.

[24] A. G. Ivanov, V. N. Mineev, E. Z. Novitskii, V. A. Yanov, and G. I. Bezrukov, JETP Lett. 2, 223 (1965).

ACKNOWLEDGMENT

The authors wish to thank Dr. E. B. Royce of the Lawrence Radiation Laboratory for informative discussions.

JOURNAL OF APPLIED PHYSICS VOLUME 37, NUMBER 7 JUNE 1966

High-Pressure Electrical Behavior and Equation of State of Magnesium Oxide from Shock Wave Measurements

THOMAS J. AHRENS

Poulter Laboratories, Stanford Research Institute, Menlo Park, California

(Received 1 December 1965; in final form 17 January 1966)

A decrease in resistivity of MgO from $>10^5$ to $\sim 10^3\,\Omega\cdot$cm is observed when thin single crystals are shocked in the [001] direction to 920±70 kbar. This effect may be produced by several electronic processes, or by ionic transport in which the effective O^- or Mg^{++} diffusion constants are increased by perhaps a factor of 10^{39} from those calculated at high pressure (according to Zener strain-energy model). Voltages are observed during passage of various-strength (70 to 936 kbar) shock fronts through the specimen. These voltages approximately scale as the inverse of the specimen thickness and may arise from net volume polarization (~0.2 to ~9 V/cm). Some Hugoniot data to 660 kbar (including measurement of elastic-shock amplitude varying from 35 to 89 kbar) are presented.

INTRODUCTION

EXPERIMENTS were performed on MgO to explore electrical resistivity, voltage generation under shock compression, and high-pressure equation of state. MgO was studied because it is simply structured (NaCl-type lattice), of technological importance, and a probable constituent of the earth's interior. (The study of electrical conductivity and equation of state of MgO at high pressure may possibly be related to studies of the earth's interior since both resistivity and elastic constants as a function of depth have been inferred from geomagnetic[1] and seismological[2] studies, respectively.)

Measurements of diffusion[3,4] of various species and electrical resistivity[5,6] in single and polycrystalline MgO at atmospheric or reduced pressures and at high temperature have been performed in differing gaseous environments. Controversy exists[5,6] as to whether the conductivity at normal pressures above 1500°K in the pure material results from primarily ionic or electronic carriers. (It has been suggested[5] that electronic conductivity is not of the extrinsic or intrinsic type usually described in semiconductors.) At sufficiently high pressure (and temperature), electronic contributions to conductivity are expected when the valence-to-conduction band gap (~9 eV at ambient pressure) is decreased. Of interest here is a calculation performed by Wada[7] which predicts metallic conductivity in MgO when the specific volume is decreased by a factor of ~0.71. Of interest to studies of shock compression is the $10^{14}/\text{cm}^3$ concentration of F centers in MgO which has been reported[8] to occur in single-crystal MgO after passage of a strong shock-wave disturbance. This result suggests that as in the case of slow deformation,[9] the shock produces copious numbers of charged defects which may give rise to a substantial (and perhaps temporary) resistivity decrease.

[1] D. C. Tozer, *Physics and Chemistry of the Earth*, edited by L. H. Ahrens, F. Press, K. Rankama, and S. K. Runcorn (Pergamon Press, New York, 1959), Vol. 3, p. 414.
[2] S. P. Clark, Jr., and A. E. Ringwood, Rev. Geophys. 2, 35 (1964).
[3] R. Lindner and G. D. Parfitt, J. Chem. Phys. 26, 182 (1957).
[4] Y. Oishi and W. D. Kingery, J. Chem. Phys. 33, 905 (1960).
[5] S. P. Mitoff, J. Chem. Phys. 36, 1383 (1962).
[6] M. O. Davies, J. Chem. Phys. 38, 2047 (1963).

ELECTRICAL MEASUREMENTS

The resistivity experiments summarized in Table I were performed using the longitudinal arrangement (current flow parallel to shock propagation direction) shown in Fig. 1, in which the MgO single crystals were mounted between a metal driver plate and a brass backing electrode. This arrangement is similar to that employed in measuring resistivity of shocked NaCl and NaCl, CsI, and KI by Al'tshuler *et al.*[10] and Doran and Ahrens,[11] respectively. A flat-topped (or nearly flat-

[7] T. Wada, Disaster Prevent. Res. Inst., Kyoto Univ. Bull. 31, 1 (1960).
[8] W. B. Gager, M. J. Klein, and W. H. Jones, Appl. Phys. Letters 5, 131 (1964).
[9] G. K. Walters and T. L. Estle, J. Appl. Phys. 32, 1854 (1961).
[10] L. V. Al'tshuler, L. V. Kuleshova, and M. N. Pavlovskii, Soviet Phys.—JETP 12, 10 (1961).
[11] D. G. Doran and T. J. Ahrens, Stanford Research Institute, Project 4100, Contract DA-04-200-ORD 1279, Final Rept., 31 Aug. 1963.

TABLE I. Resistivity and shock-induced voltage, MgO.

Shot No.	Explosive system[a] (Code)	Initial specimen thickness[b] (mm)	Shock pressure (kbar)	Particle velocity[c] (mm/μsec)	Shock-induced voltage (scaled) (V/cm)	Resistivity (Ω·cm)
11 542	A	5.0	70±5	0.744	0.212±0.009	Passive[d]
10 562	C	3.4	182±6[e]	0.59[e]	0.96 (0.48–0.96)	>4.2×10[4]
10 561	D	2.5	424±20[f]	1.31[f]	6.56±0.09	>8.3×10[4]
10 563	D	4.7	444±12[e]	1.36[e]	6.68±0.50	Passive[d]
10 887	E	3.4	660±33[f]	1.92[f]	6.25 (6.25–6.61)	∞[g]
10 888	F	2.6	798±24[h]	2.23[h]	9.09[i] (8.18–9.30)	∞[i]
10 464	G	1.9	882[f] (845–926)	2.32[f]		1.2×10[3] (0.9–1.8)
10 889	H	1.1	962±29[h]	2.60[h]	8.48±0.09[i,j]	7.3×10[3][i,j] (6.6–12.8)
10 890	H	1.1	910±27[h]	2.44[h]	8.76±0.17[i,j]	9.3×10[3][i,j] (8.0–13.2)
10 891	H	1.2	936[f] (883–991)	2.49[f]	10.21±0.29[i,j]	1.4×10[3][i,j] (1.1–2.6)
10 891	H	1.5	936[f] (883–991)	2.49[f]	8.04[i,j] (8.04–8.30)	Passive[d]

[a] See Table II.
[b] Specimen shocked in [001] direction.
[c] Inferred from Hugoniot data generated in shots 10 520, 10 724, and 11 461.
[d] Passive experiment (zero applied voltage).
[e] State in driver plate and specimen from Manganin-wire shock-pressure gauge.
[f] State in driver plate and specimen from previous determination with same explosive system.
[g] Fired in #200 Dow–Corning silicone oil.
[h] State in driver plate and specimen from driver free-surface velocity (electrical pin-contact measurement).
[i] Guardring electrode arrangement.
[j] Fired in "liquid carbonic" Grade "A" helium (99.998% He).

topped) shock wave, whose duration is at least as great as the shock travel time through the specimen, is produced in the driver plate by the impact of an explosively launched planar flyer plate or by a plane-wave-initiated thick pad of high explosive in contact with the driver plate (Table II). The resulting shock wave in the driver plate propagates into the specimen and then into the brass backing electrode. Because the latter approximately matches the specimen shock impedance, a portion of the specimen will remain in the high-pressure compressed state for a time interval which depends on both the duration of the shock pulse and the lateral specimen dimensions. The specimen is thin compared to the backing electrode or driver plate. The specimen resistivity is measured during the time that a substantial portion of the specimen is in the high-pressure state (usually before 0.5 μsec has elapsed after the shock front has left the specimen and is propagating into the backing electrode). The voltage v_x observed on the oscilloscope during this time is related to the specimen

TABLE II. Explosive and plate accelerating systems.

Code	System composition
A	$\frac{1}{4}$ in. thick aluminum projectile (speed: 0.64 mm/μsec, accelerated by gas gun) +$\frac{1}{4}$ in. aluminum
B	P-80[a,b] +2 in. Baratol[b] +$\frac{3}{4}$ in. 2024 aluminum
C	P-60[a,b] +2 in. Baratol +$\frac{3}{8}$ in. 2024 aluminum
D	P-60 +2 in. 9404[b] +$\frac{3}{8}$ in. 2024 aluminum
E	P-80 +4 in. 9404 +$\frac{1}{16}$ in. Lucite +$\frac{1}{4}$ in. tool steel +1$\frac{1}{2}$ in. air (Free-Run) +$\frac{3}{8}$ in. brass (Anaconda #238)
F	P-80 +4 in. 9404 +$\frac{1}{16}$ in. Lucite +$\frac{3}{16}$ in. tool steel +1$\frac{1}{2}$ in. air (Free-Run) +$\frac{3}{8}$ in. brass (Anaconda #238)
G	P-80 +4 in. 9404 +$\frac{1}{16}$ in. Lucite +$\frac{1}{8}$ in. stainless steel +1$\frac{1}{2}$ in. air (Free-Run) +$\frac{3}{8}$ in. 2024 aluminum
H	P-80 +4 in. 9404 +$\frac{1}{16}$ in. Lucite +$\frac{1}{8}$ in. stainless steel +1$\frac{1}{2}$ in. air (Free-Run) +$\frac{3}{8}$ in. brass (Anaconda #238)

[a] P-60 and P-80 denote 6- and 8-in.-diam explosive plane-wave generators.
[b] Manufactured by Mason and Hanger, Inc., Amarillo, Texas.

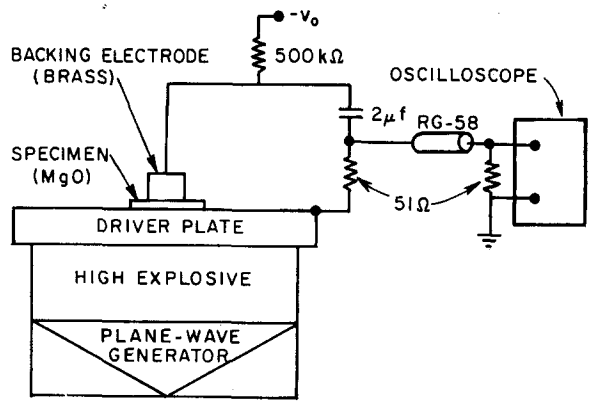

FIG. 1. Mechanical configuration and circuitry, shock resistivity experiments. (v_0 and 0 are recorded at oscilloscope when specimen resistivity approaches zero and infinity, respectively.)

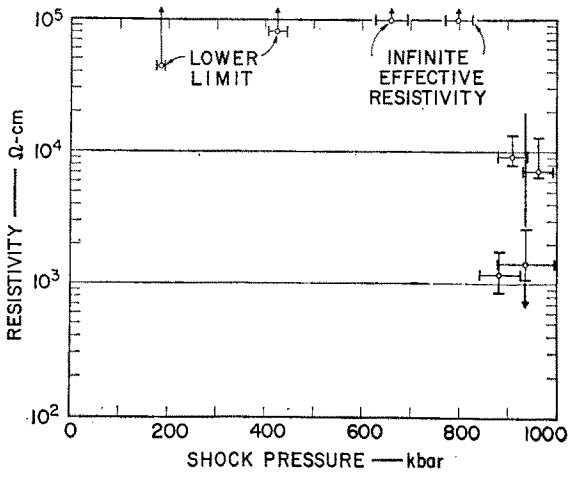

FIG. 2. Resistivity vs maximum shock pressure. (Brackets indicate estimated maximum uncertainties.)

resistivity ρ by

$$\rho=(R_0A/L)[(v_0/v_x)-1]. \quad (1)$$

Here R_0 is the effective resistance in parallel with the specimen (including cable termination), v_0 is the negative of the applied dc voltage, and L and A are the conduction path length and area, respectively. For the results quoted in Table I and Fig. 2, L is taken to be equal to the specimen thickness after shock compression and A is equal to either the cross-sectional area of the entire brass electrode or, in the case of the guardring electrodes described below, it is equal to the area of the central brass portion. For the specimen dimensions and viewing resistor used, the circuit is useful for measuring resistivities in the 10^5 to 10 $\Omega\cdot$cm range; these correspond to oscilloscope signals v_x of $\sim 0.02|v_0|$ to $\sim 0.98|v_0|$ volts. As many as six oscilloscopes, two of which had double beams, were used in each shot to record the signals at different writing speeds and sensitivity levels (Figs. 3 and 4). Oscilloscopes were triggered with a pulse originating in the electronic detonating unit which was delayed from the time of the initial explosive detonation using both an electronic and a cable system.

To exclude the possibility that the observed decrease in resistivity in the very high-pressure experiments could result from ionized air surrounding the shocked specimen, two of the shots were fired in a chamber containing free-flowing, high-purity helium. This precaution was observed even though a planar shock resulting from impact of a driver plate at 3 mm/μsec would give, in air, a shock pressure of $\sim$130 bar and a temperature of $\sim$6400°K. This shock state is only in the range in which N_2 dissociates (to form N), and no ionization is expected.[12] It was felt, however that the effect of shock convergence or even small-scale jetting at the lower edge of the specimen and electrode might result in local regions of higher pressure and perhaps of ionization. In contrast to air, a shock driven into helium by a driver plate traveling at 3 mm/μsec will produce a shock temperature of only $\sim$1450°K—ionization is not expected until the plate velocity is in the range of 7 to 8 mm/μsec. The results of the resistivity experiments fired in the helium atmosphere (Table I) were the same as those obtained in air.

In several experiments a guardring electrode made of an 0.7-mm-thick Teflon sleeve separating an inner electrode from an outer guardring of equal area was used. Two identical circuits of the type shown in Fig. 1 permitted resistivities corresponding to the inner and guardring electrodes to be obtained in a single experiment. In several shots these were observed to be very nearly equal; at the highest pressures this equality may be due to electrical conductivity in the Teflon. If the Teflon is conducting, the resistivities obtained from the inner electrode, as listed in Table I, should be increase by a factor of two.

In addition to firing the experiment in the helium atmosphere and using a guardring electrode, one shot (10 887) was fired with the specimen and backing electrode immersed in Dow–Corning silicone oil # 200 (2 centistoke). No significant resistivity decrease in the MgO was observed in this experiment. The resistivity of silicone oil was also separately tested with the same explosive system by immersing a brass electrode in the oil to provide an effective specimen thickness of 3.2 mm (thickness of oil layer between driver plate and electrode). A resistivity of $\sim$38 $\Omega\cdot$cm in the oil for a shock pressure of $\sim$164 kbar was observed (shock velocity inferred from duration of specimen-induced voltage signal, shock particle velocity obtained approximately from previously determined state in the driver plate). This result, which is inconsistent with the specimen resistivity, suggests that this oil should not be used as an insulating medium in a driver system in which the shock pressure (in brass) exceeds $\sim$600 kbar. Early experimentation[11] indicated that at a lower pressure

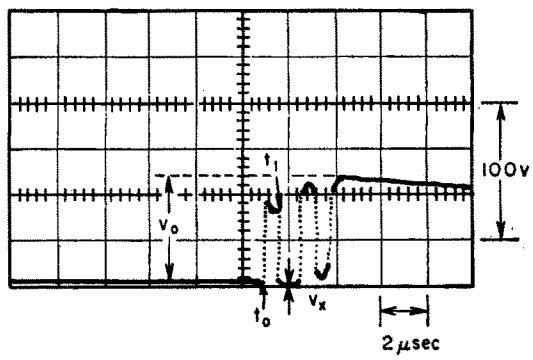

FIG. 3. Oscilloscope signal (660 kbar, shot 10 887); times t_0 and t_1 correspond to shock entering specimen and entering electrode, respectively. Resistivity is effectively infinite for period of $\sim$0.8 μsec after t_1. Short-circuiting (at first intermittent) then occurs, presumably due to driver plate moving around specimen and contacting backing electrode.

[12] J. D. Laird and K. Heron, "Shock Tube Gas Dynamic Charts," Part I, TM 64-12, AVCO, RAD Division, 10 April 1964.

(~108 kbar) silicone oil remains a relatively good insulator ($\rho > \sim 10^4\ \Omega\cdot$cm).

The shock pressures produced in the MgO specimens were obtained using Hugoniot data and knowledge of the shock state produced in the driver plates by each of the explosive or plate-impact systems. The driver plate state is obtained by: (1) measuring the driver plate free-surface velocity; (2) measuring the flyer plate velocity prior to impaction of the driver plate (shot 11 592); (3) using the Manganin wire shock-pressure transducer[13]; or (4) assuming reproducibility of the pressure produced by a given explosive system. For methods (1) and (2) electrical contactor pins set 5 and 30 mm apart were used. Using the Hugoniot curves for MgO, the driver and flyer plates, and applying the impedance-match method,[14] the final shock states in the driver plate and specimen are determined. Method (3), used for the lower pressure shots, gives the shock pressure within a block of C-7 epoxy which is in contact with the driver plate. This is obtained from the relative change of the electrical resistance of a Manganin wire imbedded in the C-7 as it becomes encompassed by the shock front. From the shock pressure in the C-7, the shock states in the driver plate and in the MgO specimen are obtained using the impedance-match method.

No account was taken of the pressure increase which results from shock reflection caused by the slight impedance mismatch at the MgO–brass interface or the pressure decrease which results from propagation of rarefaction waves inward from the lateral specimen and electrode surfaces. Both of these effects must occur, even within the 0.5 μsec during which the resistivity measurements are performed. The compression of the specimen in these experiments should be nearly one-dimensional because the driver assemblies employed generate planar shock waves and the ratio of specimen thickness to diameter is small. Hence the relative change of thickness should equal the specific volume change or

$$L/L_0 = V/V_0. \tag{2}$$

V and L are the specimen specific volume and thickness, respectively, in the shocked state and the zero subscript indicates the initial or zero-pressure value. For a single shock wave encompassing material initially at rest, with a shock velocity of U and a particle velocity of u, the specific volume is obtained from the Rankine–Hugoniot mass conservation relation

$$V = V_0(U-u)/U. \tag{3}$$

The specimens used were high-purity, single-crystal "Magnorite" supplied by Norton Co., Niagara Falls, N. Y. The crystals chosen for the electrical experiments were transparent and light brown or yellowish in appearance. Specimens approximately 30 mm square were cleaved [(001) plane] to the desired thickness and lapped with alcohol and aluminum oxide powder to ± 0.03 mm in flatness and parallelism. To assure specimen dryness after mounting the specimen in the shot assembly, the entire assembly was placed in a vacuum chamber (100 μ) and heated to ~100°C for several hours. The vacuum was retained until shortly before the experiment was fired.

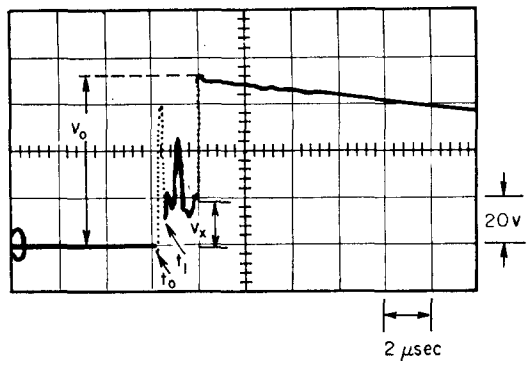

FIG. 4. Oscilloscope signal (882 kbar), shot 10 464) indicates resistivity of 0.9 to $1.8\times10^3\ \Omega\cdot$cm. (Specimen-induced signal even observed during interval t_0 to t_1 when voltage is not applied to circuit.)

Less perfect crystals were used for the Hugoniot experiments, particularly for the greater thickness specimens; the 9.7-mm-thick specimen used in shot 11 461 had several tetrahedron-shaped imperfections which appeared to be internal voids (~0.1 mm on a side). These were placed so as not to be close to the field of view of the streak camera slit.

RESULTS OF ELECTRICAL MEASUREMENTS

The resistivity obtained for MgO shows a marked and a reproducible decrease (Fig. 2) to values on the order of 1000 $\Omega\cdot$cm for shock strengths of 920 ± 70 kbar. Below that pressure level only a lower limit of the resistivity, $\sim10^5\ \Omega\cdot$cm, can be deduced from the noise level of 1 to 2 V recorded on the oscilloscope. (This noise level is also recorded after the shock front leaves the specimen in shots for which a voltage is not impressed on the circuit shown in Fig. 1.)

Although it appears impossible, from only these results, to deduce precisely the nature of the mechanism which produces the observed resistivity decrease, certain limitations—particularly on possible ionic transport processes—may be imposed from the results of normal-pressure, high-temperature experiments on MgO. At temperatures greater than 1800°K, and at both high (1 to 10^{-2} bars) and low (10^{-4} to 10^{-8} bars) oxygen partial pressure, Mitoff suggests[5] that the electrical conductivity results from electronic carriers (possibly produced by thermally activated point defects). Mitoff concludes that at lower temperatures the Mg^{++} ion is the predominant charge carrier with impurities determining electrical behavior down to 1300°K (the lower limit of his experimental range). Davies, on the other

[13] D. D. Keough, R. F. Williams, and D. Bernstein, ASME Paper 64-WA/PT-5 (1964); Trans. ASME (to be published).

[14] M. H. Rice, R. G. McQueen, and J. M. Walsh, *Solid State Physics*, F. Seitz and D. Turnbull, Eds. (Academic Press Inc., New York, 1958), Vol. 6.

TABLE III.[a] Calculated[b] shock temperature and 20°C isotherm, MgO.

Specific volume, V (cm³/g)	Hugoniot pressure, P_H (kbar)	Hugoniot temp., T_H (°K)	Adiabat[c] temp., T_A (°K)	Specific heat along Hugoniot, C_V (cal/mole °K)	20°C isotherm pressure, P_T (kbar)
0.2717	42.9	307	307	3.775	42.2
0.2637	96.1	323	321	3.793	94.8
0.2558	163	345	336	3.848	161
0.2478	247	375	352	3.959	243
0.2398	354	419	369	4.150	349
0.2319	493	485	386	4.417	484
0.2239	674	584	405	4.737	660
0.2159	917	733	424	5.060	895
0.2080	1248	959	444	5.361	1212
0.2000	1710	1313	465	5.595	1653

[a] Based on Table IV data.
[b] Constants assumed in calculations: $\gamma_0=1.62$, $V_0=0.2796$ cm³/g, $\theta_0=931$°K, $T_0=293$°K, $C=6.15\times10^5$ cm/sec, and $S=1.85$.
[c] Adiabat passing through $P=0$, $V=V_0$.

hand, concludes[6] that at both high and low temperatures conductivity results from either Mg^{++} or $O^{=}$ transport, depending again upon oxygen pressure and, at lower temperatures, impurity level.

It is interesting to compare the resistivities obtained in ambient-pressure, high-temperature experiments with those obtained in the present shock experiments. At the shock pressure level at which the MgO resistivity decreases to 1000 Ω·cm (specifically 917 kbar, Table III) a shock temperature of 733°K is calculated. In contrast to the shock wave result, this same resistivity (~1000 Ω·cm) is achieved only at ~2200°K at ambient pressure. (This temperature is inferred from an extrapolation of Mitoff's resistivity data[5] by two orders of magnitude in resistivity.) One may also compare the shock resistivity (at 917 kbar and 733°K) with the resistivity value that might be measured at ambient pressure and 733°K. By extrapolating the ambient-pressure resistivity data to lower temperatures, an upper bound of 10^{14} Ω·cm at ~733°K is obtained. This result is valid only if charge transport processes with the same activation energy as at ~1300°K remain dominant down to 733°K.

From these comparisons it may be concluded that the low resistivity observed at a fairly low temperature under shock compression is not due to the same temperature-dependent ionic or perhaps electronic processes as those observed at essentially zero pressure, but instead involves processes which may be unique to the high pressure and severe deformation encountered by the shocked MgO.

One possible mechanism which may give rise to the observed resistivity decrease is electronic conduction, either extrinsic from impurity-produced energy levels lying between the valence and conduction band (normally separated by ~9 eV), or intrinsic from a pressure-induced reduction in the energy gap between the valence and conduction band. Verification of the dominance of either of these processes requires additional resistivity shock experimentation and perhaps such other types of measurements as determinations of the optical properties of MgO in the shocked state. A calculation of the effect of compression on the electronic band structure of MgO is reported by Wada.[7] He finds that the conduction and valence band of MgO overlap when the lattice spacing is reduced to 1.87 Å (V_0/V is 1.415). This compression is greater than that achieved in these shock experiments, and extrapolating the Hugoniot data (described below) it would be achieved at somewhat greater than 2000 kbar. This may be compared with the 1030 kbar which Wada obtained by evaluating a Born–Mayer type of equation of state.

The observed resistivity decrease may also be due to an ionic transport mechanism. For this case it is possible to set a firm lower limit on the diffusion constant of the dominant charge transport process which gives rise to the resistivity decrease. This is accomplished by demanding that the total number of carriers per unit volume, n, does not exceed the total number of atoms per unit volume, n_0. Using the Nernst–Einstein equation

$$D=kT/\rho n(z_ie)^2, \tag{4}$$

where D is the self-diffusion constant, z_ie the magnitude of the electrical charge of the appropriate carrier, ρ the resistivity, and kT has the usual meaning, we demand that

$$D\geq kT/\rho n_0(z_ie)^2. \tag{5}$$

Taking a value of shock temperature of 733°K at 917 kbar (Table III), Eq. (5) gives for $\rho=10^3$ Ω·cm,

$$D\geq 10^{-9}\ \text{cm}^2/\text{sec}. \tag{6}$$

Here z_ie is nominally taken as two electronic charges. Values of the diffusion constant for Mg^{++} and $O^{=}$ of 6×10^{-25} and 5×10^{-25} cm²/sec may be calculated at 733°K from the data of Lindner and Parfitt[3] and Oishi and Kingery,[4] respectively. These values substituted into Eq. (4) both result in $n\cong2\times10^{33}$/cm³ carriers at 733°K. This value far exceeds both n_0 and the minimum number of vacancies (actually ~10^{14}/cm³ F centers) found to be present in explosively shocked MgO which has been recovered after exposure to high shock pressure. It is expected that the diffusion constant used

in Eq. (4) should be markedly decreased by high pressure.

An estimate of the effect of pressure on the diffusion constant of an ionic species may be obtained by applying at least one of the theoretical treatments of the effect of pressure on activated processes presented by Keyes.[15] The diffusion constant may be written as

$$D = fa^2\nu e^{-\Delta G^*/kT}, \tag{7}$$

where f is a geometrical factor, a is the lattice spacing, ν is the vibrational frequency of the carrier, and ΔG^* is the appropriate Gibbs activation energy for the diffusion process. ΔG^* may include the energy required to create a vacancy in addition to that required for an ion and vacancy to interchange positions. The pre-exponential factor in Eq. (7) may be written

$$fa^2\nu = gV^{2/3-\gamma}, \tag{8}$$

where g is a constant and γ is Grüneisen's ratio. Equation (8) results from assuming that the carrier vibration frequency is proportional to the Debye temperature and hence $V^{-\gamma}$. Differentiating Eq. (7) with respect to pressure at constant temperature gives

$$(d\ln D/dP)_T \cong [(\tfrac{2}{3}-\gamma) + (\Delta G^*/kT)(2\gamma-\tfrac{2}{3})](d\ln V/dP)_T, \tag{9}$$

where g is assumed not to vary appreciably with P and

$$(d\Delta G^*/dP)_T = -\Delta G^*(2\gamma-\tfrac{2}{3})(d\ln V/dP)_T. \tag{10}$$

Equation (10) follows from Eqs. (4)–(9) and (4)–(21) of Keyes treatment of Zener's strain-energy model. Since the value of $\Delta G^*/kT \gtrsim 43$ for diffusion of Mg^{++} or $O^=$ below 10^3 °K in MgO, the first term in the bracket in Eq. (9) is neglected since generally, $\gamma \gtrsim \frac{1}{3}$. Equation (10) may be integrated to give the Gibbs activation energy as a function of compression along an isotherm as

$$\Delta G^* = \Delta G_0^*(V_0/V)^{(2\gamma-\frac{2}{3})} \tag{11}$$

or

$$\Delta G^* = \Delta G_0^*[e^{2\gamma(V_0-V)/V} + (V/V_0)^{\frac{2}{3}}]. \tag{12}$$

Equations (11) and (12) are obtained by assuming either γ or $\gamma/V(\equiv b)$ are constant along an isotherm. ΔG_0^* denotes the Gibbs activation energy at zero (ambient) pressure. Substitution of Eqs. (11) and (12) into Eq. (9) (with the first term in the bracket deleted) and integration yield

$$D \cong D_0 \exp\{-\Delta G_0[(V_0/V)^{(2\gamma-\frac{2}{3})}-1]/kT\} \tag{13}$$

or

$$D \cong D_0 \exp\Big(-\Delta G_0\Big\{(V/V_0)^{2/3} + e^{2b(V_0-V)} - 2 - 6b[V(V/V_0)^{2/3} - V_0]/5 - 2e^{2bV_0/3}\Big[\ln(V_0/V) + \sum_{n=1}^{\infty}(-2b)^n(V_0^n - V^n)/n\cdot n!\Big]\Big\}/kT\Big), \tag{14}$$

where γ and $\gamma/V = b$ are again considered constant for Eqs. (13) and (14), and D_0 is the observed diffusion constant at zero pressure. Equation (13) yields the values of 10^{-61} and 10^{-70} cm²/sec for $O^=$ and Mg^{++} diffusion, respectively, at a compression (V/V_0) and temperature of 0.772 and 733°K. Equation (14) yields values of D of 10^{-48} and 10^{-55} cm²/sec for $O^=$ and Mg^{++} diffusion, respectively. All these values violate the condition of Eq. (6).

Although the carrier multiplication mechanism appears to account for the decrease in resistivity observed in the slow deformation experiments on alkali halides performed by Camagni and Manara,[16] in the present experiments an unreasonably high carrier density, which would be in fact far greater than the number of atoms per unit volume, would be required. It may be concluded from this argument that for ionic conductivity of the magnitude observed, the effective diffusion constant of the appropriate ionic species must be greatly enhanced under shock, by perhaps 39 or more orders of magnitude, over that predicted under high pressure by the Zener strain-energy models. It may be that such a radical increase in diffusion constant actually occurs and is the same as or closely related to the so-called pipe diffusion observed in deformed LiF.[17] Undoubtedly a large number of dislocations, which also give rise to vacancies, are produced by the passage of the shock front. In this case the preferred orientation of dislocations might be expected to be parallel to the shock front. If ionic transport along a dislocation pipe was an important conduction mechanism, a lower resistivity parallel to the shock front than perpendicular to it would be expected. It is interesting and probably meaningful that such a relation was indeed observed in the shock-resistivity experiments performed on CsI and KI.[11,18]

SPECIMEN-INDUCED VOLTAGES

In addition to signals resulting from the decrease in MgO resistivity, signals with amplitudes varying from +1.2 to +105 V (at shock strengths varying from 70 to 936 kbar) appear across the viewing resistor (Fig. 1) during the time that the shock fronts are propagating through (within) the specimen. The excitation which produced these voltages is believed to originate within the specimen, since in several shots (e.g., shots 10 561 and 10 563) essentially identical signals are observed when no dc voltage (v_0) is impressed.

As in the case of shock propagation through alkali halides in which a similar effect is observed,[19] the dura-

[15] R. W. Keyes, in *Solids under Pressure*, W. Paul and D. M. Warschauer, Eds. (McGraw-Hill Book Co., Inc., New York, 1963).

[16] P. Camagni and A. Manara, J. Phys. Chem. Solids **26**, 449 (1965).

[17] R. Tucker, A. Lasker, and R. Thompson, J. Appl. Phys. **34**, 445 (1963).

[18] D. G. Doran and W. Murri, Bull. Am. Phys. Soc. II, **9**, 728 (1964).

[19] R. K. Linde, W. Murri, and D. G. Doran, J. Appl. Phys. **37**, 2527 (1966) (this issue).

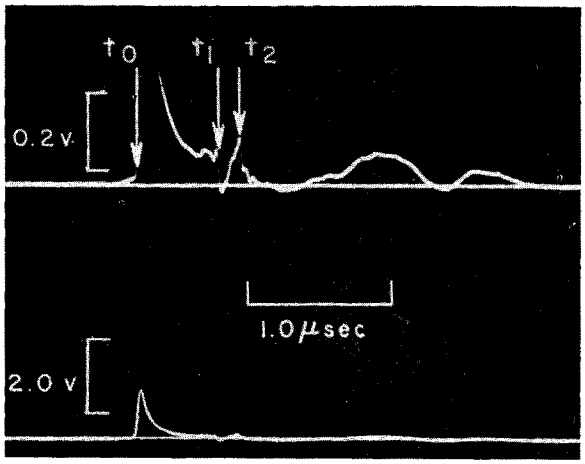

FIG. 5. Specimen-induced signal, final shock state (70±5 kbar, shot 11 542). (No voltage applied to circuit.) Times t_0, t_1, and t_2 apparently correspond to entrance of shock into specimen, exit of elastic shock from specimen, and exit of deformational shock from specimen. These times give ~9.5 and ~7.4 mm/μsec for elastic and deformational shock velocity. See Table IV.

tion of these specimen-induced signals corresponds closely (±0.03 μsec) with the estimated transit time of either the elastic or deformational shock through the specimen (at high pressure the time resolution does not permit differentiation between these two). In one lower pressure shot (11 592) in which a thick specimen was used, the difference in velocity between the elastic and the following deformational shock permitted sufficient time resolution of the specimen-induced voltage so that signal features could be correlated with the elastic and deformational shock transit times. It is interesting that changes in signal amplitude are observed at times which correspond closely to exit of both the elastic and deformational shocks from the specimen (Fig. 5).

The specimen-induced voltages from the guardring electrode experiments (only the center electrode results are quoted) and those using solid electrodes are given in Table I. As suggested by Allison[20] and Hauver,[21] the voltage observed when the shock enters the specimen (which, when resolved in these experiments, was the maximum voltage) may be scaled by multiplying by the initial specimen thickness and dividing by the specimen or, in this case, electrode area (Table I and Fig. 6). In the case of the approximately 1-mm-thick specimens, systematic errors in the measurement of the specimen-induced voltage (duration of ~0.1 μsec) were probably present because of the inductance in the cables leading to the oscilloscopes. The specimen-induced voltages appearing across the outer guardring electrode were found to be as much as 90% greater (shot 10 890) than those generated at the center electrode. This latter effect, as well as the general variation with shock strength and the association of different signals with both the elastic and deformational shock front (shot 11 542), suggest that these specimen-induced voltages result from the net displacement of charged defects (produced by the shock deformation) in the specimen material. The scaling law suggested by Allison and Hauver supplies what appears to be an adequate ordering to the data and is consistent with a model for which the voltages observed are produced by net volume polarization of the shocked MgO (dipoles oriented in the direction of shock propagation).

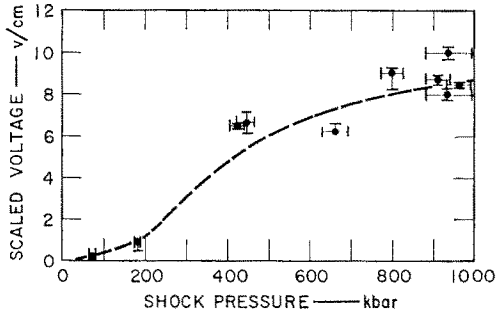

FIG. 6. Maximum specimen-induced voltage (scaled) versus shock pressure. (Brackets indicate estimated maximum uncertainty. Scaled by multiplying by specimen thickness and dividing by electrode area. Systematic voltage errors [not indicated by bracket] probably exist at high pressures because of cable inductance.)

[20] F. E. Allison, J. Appl. Phys. **36**, 2111 (1965).
[21] G. E. Hauver, J. Appl. Phys. **36**, 2113 (1965).

HUGONIOT DATA, MAGNESIUM OXIDE

Three plane-wave, inclined-mirror (streak camera) shock experiments,[22] on magnesium oxide provided Hugoniot pressure–volume data at the 170-, 420-, and 660-kbar pressure levels (Table IV and Fig. 7). These experiments were performed primarily so that the pressures achieved in the magnesium oxide in the shock-resistivity experiments could be estimated from measured shock states in the driver plates. Flat and inclined mirrors were employed to measure: (a) the transit

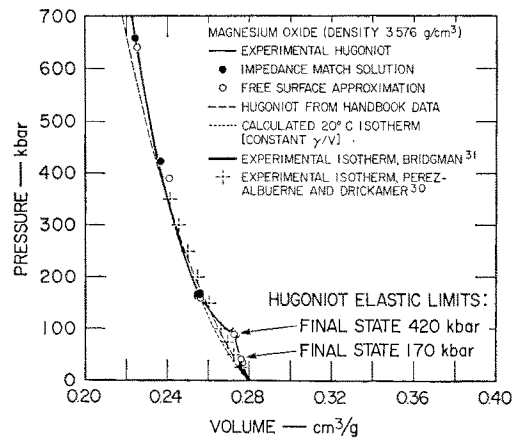

FIG. 7. Hugoniot and isotherm data, MgO. (Bracket about 89 kbar elastic limit indicates unusually large uncertainty in particle velocity.)

[22] D. G. Doran, in *High Pressure Measurement*, A. A. Giardini and E. C. Lloyd, Eds. (Butterworths Scientific Publications, Washington, 1963).

TABLE IV. Hugoniot data, MgO.[a]

Shot no.	Explosive driver system[b]	Specimen thickness, d (mm)	Elastic shock: Shock velocity, U_1 (mm/μsec)	Elastic shock: Particle velocity,[c] u_1 (mm/μsec)	Elastic shock: Pressure, P_1 (kbar)	Elastic shock: Volume, V_1 (cm³/g)	Deformational shock: Shock velocity, U_2 (mm/μsec)	Deformational shock: Particle velocity,[d] u_2 (mm/μsec)	Deformational shock: Free-surface velocity, u_{2fs} (mm/μsec)	Deformational shock: Pressure, P_2 (kbar)	Deformational shock: Volume, V_2 (cm³/g)
11 461	B	2.5	8.905±0.059	e	e	e	6.893	0.633	1.256	166	0.2546
		3.7	9.191±0.104	0.1215±0.008	39.9	0.2760	7.016	0.626	1.348	168	0.2558
		5.6	e	e	e	e	7.085	0.632	1.195	166	0.2554
		9.7	9.142±0.011	0.1054±0.011	34.5	0.2764	6.964	0.635	1.217	166	0.2551
10 520	D	2.9	f	f	f	f	7.881	1.229	2.678	390	0.2457
		7.6	10.068	0.2476	89±10	0.2728	8.593	1.35	2.459	423	0.2367
10 724	E	6.5	g	g	g	g	9.61	1.92	3.733	660	0.2239

[a] Initial density = 3.576 g/cm³.
[b] See Table II.
[c] $u_1 = u_{fs1}/2$, assumed.
[d] Impedance match solution (see Ref. 14).
[e] Elastic shock, not successfully recorded.
[f] Experiment not designed to observe elastic shock.
[g] Elastic shock presumably overdriven.

times of both the elastic (first) and deformational (second) shock fronts through the specimens; (b) the free-surface velocities imparted by the incident shock to the driver plate; and (c) the free-surface velocities of the specimen resulting from internal reflection of the elastic and deformational shocks. The elastic shock state was computed assuming that the free-surface velocity equals twice the shock-particle velocity; the second or deformational shock state was computed using the impedance-match method.[14] To obtain the deformational (second) shock velocity (U_2) when two shock fronts are present, the interaction of the elastic wave—which has reflected from the specimen's free surface—with the oncoming deformational shock must be taken into account. The resulting value of U_2 was found to be insensitive to the details of this interaction; therefore, for simplicity, an elastic interaction was assumed. In this case the apparent velocity

$$\bar{U}_2 = \frac{L_0 + (t_2 - t_1)u_{1fs}}{t_2 - t_0} \tag{15}$$

is related to the deformation shock velocity by

$$U_2 = \frac{3U_1\bar{U}_2 - U_1^2 - 2u_1^2 - 3u_1U_1}{\bar{U}_2(U_1+u_1)/U_1 + U_1 - 4u_1 - 2u_1^2/U_1}. \tag{16}$$

Here u_{1fs} is the specimen free-surface velocity resulting from interaction of the first shock with the free surface. The errors in determining the shock and particle velocities in these shots are believed to be less than 1% and 3%, respectively. The agreement between the (final state) particle velocities obtained from taking one-half the specimen free-surface velocities and those deduced from the driver plate free-surface velocities using the impedance-match method (Table IV) implies that the shock and subsequent rarefaction are nearly reversible.

Of special interest is the elastic-shock amplitude (Table IV) which is markedly dependent on both the final shock state and, possibly to a lesser extent, on specimen thickness at a constant final shock state. The elastic-shock amplitude increases (35 to 89 kbar) with increasing final shock pressure (166 to 423 kbar); also, the elastic-shock amplitude decreases with increasing shock propagation path length (40 to 35 kbar, 4.7 to 9.7 mm, at final shock state of 166 kbar). Both of these effects suggest that the shear stress in MgO, under one-dimensional compression, decreases with time. This behavior is similar to the stress-relaxing solid discussed by Duvall.[23]

In order to facilitate the calculation of temperatures existing within the shocked MgO in the high-pressure state (corresponding to conditions under which the resistivity measurement is performed), the Hugoniot data were fit to the line[24]

$$U^* = C + Su^*, \tag{17}$$

where C and S are constants. U^* and u^* are either the shock and particle velocity associated with a single shock front or, in the pressure range where two shock fronts are present, the equivalent shock and particle velocity which would correspond to the final (deformational) shock state being achieved by a single shock front. Thus in the case of two shocks

$$u^* = [P_2(V_0 - V_2)]^{\frac{1}{2}} \tag{18}$$

$$U^* = V_0[P_2/(V_0 - V_2)]^{\frac{1}{2}}, \tag{19}$$

where, as usual, the subscripts refer to the first and second shock fronts. From a mean square fit of seven datum points, reduced according to Eqs. (18) and (19), $C = 6.15$ mm/μsec and $S = 1.85$.

By applying the Rankine–Hugoniot relations for a single shock to Eqs. (18) and (19), the Hugoniot pressure–volume relation may be written

$$P_H = C^2(V_0 - V)/[V_0 - S(V_0 - V)]^2, \tag{20}$$

where P_H is now used for the pressure along the Hugoniot.

In order to calculate shock temperature T_H, the following formula (first derived by Walsh and Christian[25]) giving the temperature along the Hugoniot, is applied:

$$T_H = T_0 e^{b(V_0 - V)} + e^{-bV}\int_{V_0}^{V} \{e^{bV}[(V_0 - V)(dP/dV) + P]dV/2C_V\}_{\text{Hug.}} \tag{21}$$

[23] G. E. Duvall, in *Stress Waves in Anelastic Solids*, H. Kolsky and W. Prager, Eds. (Springer-Verlag, Berlin, 1964).
[24] J. Wackerle, J. Appl. Phys. 33, 922 (1962).
[25] J. M. Walsh and R. H. Christian, Phys. Rev. 97, 1544 (1955).

A small and probably negligible error is introduced because the integration is not performed along the experimental Hugoniot curve but along the locus of final shock states which would be achieved by a hypothetical single shock transition. C_V is the specific heat at constant volume and again $b=\gamma/V$ is assumed constant. Because of the high value of the Debye temperature of MgO (931°K) relative to both room and shock temperatures,[26] it is desirable to use a temperature and volume-dependent form for C_V. The temperature dependence of the specific heat was assumed to be given by the Debye formula:

$$C_V=3k\left[12(T/\theta)^3\int_0^{\theta/T} y^3dy/(e^y-1) -3\theta/T(e^{\theta/T}-1)\right]. \quad (22)$$

The variation of Debye temperature θ with compression is given by

$$\theta=\theta_0e^{\gamma(V_0-V)/V}=\theta_0e^{b(V_0-V)}, \quad (23)$$

where the γ parameter of the Debye theory is now associated with the thermodynamic Grüneisen's ratio $V(dP/dE)_V$.

Equations (21), (22), and (23) were simultaneously solved numerically for T_H (Table III) with the aid of a digital computer, using the experimentally determined values of C and S in Eq. (20). It should be noted that the first term in Eq. (21) gives the temperature T_A at a specific volume V on the isentrope passing through the foot of the Hugoniot ($P=0$, $V=V_0$). The 20°C isotherm points are calculated from the relation

$$P_T=P_H-b\int_{T_0}^{T_H} C_VdT, \quad (24)$$

where C_V is obtained from Eq. (22) and the value for θ is obtained at each specific volume using Eq. (23). The calculations presented in Table III indicate that over the pressure range of the experimental data the difference between the calculated 20°C isotherm and the Hugoniot is negligible. Although the Hugoniot calculated from the values of C and S obtained from handbook data tabulated by McQueen *et al.*[27] agrees fairly closely with the experimental Hugoniot to at least 500 kbar, extensive shock-wave measurements recently performed at Los Alamos Scientific Laboratory give values of C and S more consistent with the lower pressure values of 6.9 mm/μsec and 1.3, respectively.[28,29] The agreement of the experimental isotherm of Perez–Albuerne and Drickamer[30] with the Hugoniot curve at high pressures (about 300 kbar) is satisfactory. It is not clear whether the apparent divergence of the Hugoniot data at low pressures[31] from the experimental isotherm is of particular significance except that, as in the case of quartz,[24] a positive pressure offset of the deformational Hugoniot from the hydrostatic isotherm expected for an elastic–plastic material appears to be absent. This result implies a fluid-like behavior of MgO in the deformational shock state.

SUMMARY AND CONCLUSIONS

A decrease in the resistivity of Norton "Magnorite" MgO (shocked along [001]) from $>10^5$ to $\sim10^3$ $\Omega\cdot$cm is observed at a shock pressure of 920±70 kbar. The specimens (thicknesses 1 to 5 mm) were mounted between a metal driver plate and a brass backing electrode (the latter approximately matches the MgO shock impedance). A plane shock wave is driven into the driver plate; this wave propagates through the specimen and then into a brass backing electrode. While the shock is propagating in the backing electrode, the specimen (which is thin compared with the thicknesses of both the driver plate and backing electrode) is assumed to remain at a nearly steady pressure value. The resistivity is obtained by measuring, with fast-writing oscilloscopes, the current discharged from a capacitor through the specimen within the first 0.5 μsec after the shock enters the backing electrode.

Most of the experiments were performed in air, but several shots performed in helium atmosphere gave similar results. The results were likewise unchanged by substituting guardring backing electrodes in place of the solid ones.

The observed resistivity decrease may be due to electrons arising from: (a) impurities producing donor and acceptor energy levels; (b) a compression-induced reduction in band gap; or (c) electron production by an unknown mechanism. On the other hand, the decrease may occur because of enhanced conductivity by ions. Although an increase in ionic carrier density probably results from passage of the shock, the estimates of Mg^{++} and $O^{=}$ diffusion constants obtained from the Zener strain-energy model[15] (assuming either γ or γ/V is constant) imply that it is impossible to account for the decreased resistivity solely on this basis. Pipe transport along dislocations[17] or perhaps another process is required to increase by a factor of 10^{39} the effective diffusion constants if the observed conductivity is to be attributed to ion motion. Pipe transport along dislocations might result in a lower resistivity parallel to the shock front than perpendicular to it. (Such an effect may actually be observed in KI and CsI.)[11,18]

Signals (presumably specimen-induced) whose durations correspond closely to the time that the shock fronts are propagating through the specimen and whose amplitudes are independent of the impressed dc voltage

[26] O. L. Anderson, J. Phys. Chem. Solids **24**, 909 (1963).
[27] R. G. McQueen, J. N. Fritz, and S. P. Marsh, J. Geophys. Res. **69**, 2947 (1964).
[28] R. G. McQueen, Los Alamos Scientific Laboratory (private communication).
[29] F. Birch, Harvard University (private communication).
[30] E. A. Perez-Albuerne and H. G. Drickamer, J. Chem. Phys. **43**, 1381 (1965).
[31] P. W. Bridgman, Proc. Am. Acad. Arts Sci. **77**, 187 (1949).

were recorded in all the electrical experiments. The maximum observed voltages varied from +1.2 to +105 V as the shock strength was increased from 70 to 936 kbar. An impressive ordering of these data occurs if the observed voltages are multiplied by specimen thicknesses and divided by electrode areas.[20,21] This results in scaled voltages of ~0.2 to ~8.5 V/cm over the experimental range. Such a scaling law would apply if a net volume polarization, perhaps arising from net displacement of charged defects, were present in the shocked MgO.

Hugoniot data to 660 kbar were measured and used to obtain shock pressures in the electrical experiments. Shock temperatures and a 20°C isotherm for MgO were calculated by using the Walsh and Christian formulation.[25] A constant value of γ/V and a temperature and volume dependence for C_V given by the Debye theory were incorporated into the Walsh and Christian treatment. The calculated shock temperature at the pressure level of the observed resistivity decrease is 733°K (at 917 kbar). The calculated pressure offset between the 20° isotherm (which agrees closely with that measured by Perez-Albuerne and Drickamer[30] at 300 kbar) and the Hugoniot is negligible over the experimental range (e.g., 14 kbar at 674 kbar). At lower pressure (168 kbar) the lack of a pressure offset of the deformational Hugoniot curve from the hydrostat indicates a fluid-like behavior for MgO shocked above the Hugoniot elastic limit. The value of Hugoniot elastic limit (elastic-shock amplitude) is markedly dependent (values from 35 to 89±10 kbar are observed) on the value of the final shock state (166 to 473 kbar) and to a lesser extent on shock propagation path length.

ACKNOWLEDGMENTS

This research was solely supported by the Institute Research and Development funds of Stanford Research Institute. It is a pleasure to thank my colleagues, Dr. D. G. Doran, Dr. W. Murri, Dr. G. R. Fowles, Dr. R. K. Linde, Dr. Y. Syono, and Dr. S. Gill, as well as Dr. M. O. Davies of the Lewis Research Center, for significant contributions and helpful discussion. The assistance of M. Ruderman in carrying out the Hugoniot measurements is appreciated.

JOURNAL OF APPLIED PHYSICS VOLUME 37, NUMBER 7 JUNE 1966

Computation of Electrostatic and Rapidly Pulsed Magnetic Fields*

H. R. Lewis, Jr.
Los Alamos Scientific Laboratory, University of California, Los Alamos, New Mexico
(Received 3 January 1966; in final form 18 February 1966)

It is often required, for example, in the design of some pulsed controlled-thermonuclear-fusion experiments, to calculate electrostatic fields and to calculate magnetic fields in the approximation that flux does not penetrate metal boundaries of the experimental volume. Computation of such magnetic and electric fields by means of the standard relaxation methods is often difficult and very costly, even with high-speed computers. This is because the boundaries of the region of experimental interest are rather arbitrary and because there are generally current- or charge-carrying conductors within the region that make it nonsimply connected. An alternative method of solving the boundary value problems that determine these electric and magnetic fields, which does not involve a difference approximation to the differential equations, has been developed. With this method, an exact analytic solution of the appropriate differential equation is obtained in the region of interest, and this solution is made to approximate the boundary conditions. The method and its application are described in detail. Examples of the application of the method to some controlled-thermonuclear-fusion experiments are given.

A PROBLEM that sometimes occurs in the design of physics experiments—for example, with certain plasma physics experiments for controlled-thermonuclear-fusion research—is that of computing electrostatic fields and rapidly pulsed magnetic fields. If all of the sources of the electric or magnetic field are known in advance, then it is a simple matter to write an explicit integral expression for the field in terms of those sources, even though it may not be simple to evaluate the expression numerically. However, if the sources are not all known in advance, as is the case when conductors are charged to specified potentials or when external currents in the neighborhood of conductors are rapidly pulsed, then the field is calculated by solving the appropriate boundary value problem.

For the electric and magnetic problems which we consider, the charges or currents are static and confined to conductors, either axial or translational symmetry is assumed, and there is a scalar function from which the field can be derived. The goal is to obtain an expression for the field in a region, denoted by the symbol R, which does not contain any sources whose strengths are not specified in advance. There may be some sources whose strengths are specified in advance, and any of

* Work performed under the auspices of the U. S. Atomic Energy Commission.